

RESEARCH

Open Access



Reversal of epithelial to mesenchymal transition in triple negative breast cancer through epigenetic modulations by dietary flavonoid Galangin and its combination with SAHA

Snehal Nimal¹, Navanath Kumbhar¹, Manasi S. Pote¹, Rahul Bankar², Mahemud Shaikh² and Rajesh Gacche^{1,3*}

Abstract

Background TNBC is an aggressive metastatic cancer that poses considerable treatment challenges because of its acquired drug resistance towards the existing targeted and hormonal therapies. The epigenetic modulation including HDACs triggers the EMT in TNBC which produces a more aggressive tumor phenotype. Chemotherapy and radiotherapy cause severe side effects which make treatment complex and challenging. To avoid these serious side effects and boost the effectiveness of current anti-cancer medications, plant flavonoids have been investigated.

Aim of the study The present investigation is aimed to understand the role of dietary flavonoid Gal in the modulation of epigenetic regulators such as HDACs and HATs and their impact on the reversal of the EMT process in TNBCs.

Methodology Here, we have examined the anti-TNBC potential of Gal alone and in combination with SAHA by performing series of in vitro cell culture assays such MTT, migration and invasion, cell cycle regulation, ROS generation & mitochondrial dysfunction, nuclear fragmentation & apoptosis induction etc. The expression profiles of epigenetic regulators, apoptosis regulating proteins, and EMT markers were analysed by performing transcriptomic and proteomic studies. The in vivo efficacy of Gal was studied using BALB/c mice xenograft model studies.

Results At $IC_{50} = 50 \mu\text{M/mL}$, Gal significantly inhibited the cell proliferation, migration, and invasion, arrested cell cycle at sub G0/G1 phases, generated ROS, reduced MMP and induced apoptosis in MDA-MB-231. Transcriptomic, proteomic, and calorimetric analysis revealed that Gal has potential to downregulate the expression of HDAC1/HDAC3 and elevate the expression levels of HAT. Gal also modulated the process of EMT by downregulating the mesenchymal markers and upregulating the epithelial marker. The synergistic mechanism of Gal and SAHA against the TNBCs was elucidated by understanding the expression levels of epigenetic regulators & EMT markers. Interestingly, Gal increased the expression of tumour suppressor protein pTEN and suppressed the expression of AKT,

*Correspondence:

Rajesh Gacche

rngacche@unipune.ac.in; gaccheraju53@gmail.com

Full list of author information is available at the end of the article

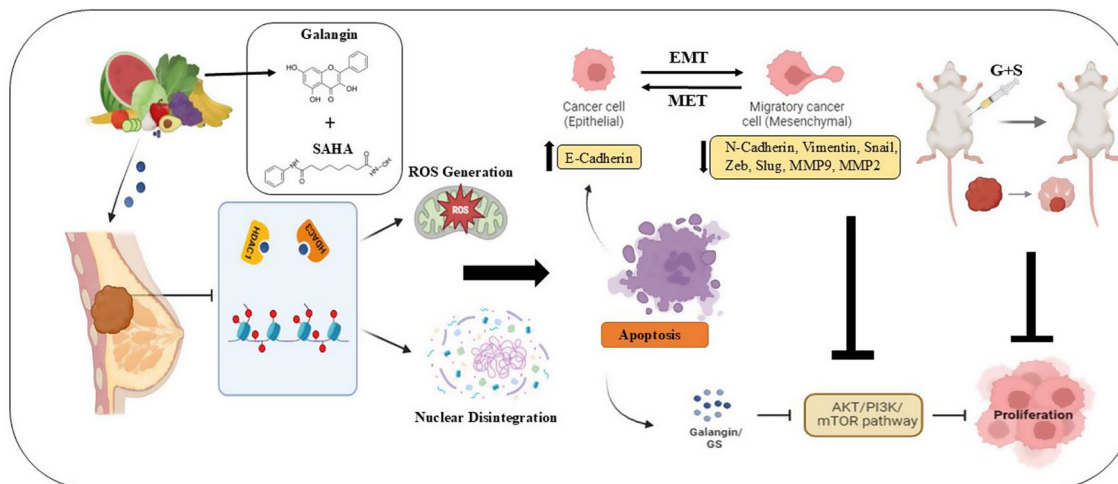


© The Author(s) 2025. **Open Access** This article is licensed under a Creative Commons Attribution-NonCommercial-NoDerivatives 4.0 International License, which permits any non-commercial use, sharing, distribution and reproduction in any medium or format, as long as you give appropriate credit to the original author(s) and the source, provide a link to the Creative Commons licence, and indicate if you modified the licensed material. You do not have permission under this licence to share adapted material derived from this article or parts of it. The images or other third party material in this article are included in the article's Creative Commons licence, unless indicated otherwise in a credit line to the material. If material is not included in the article's Creative Commons licence and your intended use is not permitted by statutory regulation or exceeds the permitted use, you will need to obtain permission directly from the copyright holder. To view a copy of this licence, visit <http://creativecommons.org/licenses/by-nc-nd/4.0/>.

PI3K, and mTOR proteins involved in the cancer proliferation pathway. Gal also demonstrated impressive antitumor effect under in vivo settings.

Conclusion In-vitro and In vivo studies confirmed Gal's potent anticancer efficacy and highlighted its potential as a promising therapeutic agent that possibly can be used with conventional chemotherapy against TNBC.

Graphical Abstract



Keywords TNBC, HDACs, Flavonoids, EMT, PI3K/AKT/mTOR pathway and in-vivo

Introduction

Breast cancer (BC) is the second greatest cause of mortality in women according to the American Cancer Society, with an increasing prevalence each year. Targeted therapies for patients diagnosed with estrogen, progesterone and HER-2 receptors are improved but the major barrier is for the patients lacking these receptors [1]. Triple negative breast cancer (TNBC) is an aggressive subtype which accounts for 15–20% of breast cancer population which is defined by the absence of estrogen, progesterone, and human epidermal growth factor receptors. It has high recurrence rates, a low survival rate, and its heterogeneity makes it a challenging and is the unmet need of the hour to develop novel, effective and safe treatment modalities against TNBC [2]. The rate of distant metastasis in TNBC patients is the highest as compared to other subtypes of breast cancer [1]. In the entire lifespan, it is predicted that one in 10 women will suffer with breast cancers and around 15% will develop TNBC [3]. A well-defined treatment approaches are limited to chemotherapy, radiotherapy, and surgery and still irrecoverable with current prescribed conventional therapies. The toxicity of these prescribed chemotherapy drugs is very harmful and do not free from side effects. Therefore, to develop novel therapeutic agents would be an inordinate clinical achievement in therapeutic management of TNBC [1].

Cancer was initially thought to be a hereditary illness, but it now includes both genetic and epigenetic

aberrations [4]. Epigenetic modifications in cancer are known to contribute to tumour formation, but can be reversed in somatic cells, leading to tailored cancer treatment options [5]. Many gene abnormalities in cancer are caused by epigenetic modifications that alter gene expression profiles, rather than change in sequences [6]. Epigenetic changes, such as DNA methylation and histone modifications, have a significant role in regulating oncogene and tumor suppressor gene expression levels in breast cancer [7]. Histone acetyltransferases (HATs) and histone deacetylases (HDACs) play a crucial role in regulating gene expression by modifying the acetylation status of histone proteins. These modifications influence the chromatin structure, either maintaining it in a “relaxed” state that facilitates gene expression or in a more compact form that suppresses it [8]. Hence various covalent modifications may interfere with or improve histone tail interactions with DNA and other proteins [4]. Understanding these modification's deregulation of HDAC activity in malignancies supports the clinical use of HDAC inhibitors, these inhibitors have shown to inhibit cell cycle, differentiation, and induce apoptosis at concentrations that leave normal cells relatively unaffected [4]. Recent research indicates that upregulation of individual HDACs is linked to poor clinical outcomes in individuals with colorectal, hepatocellular, prostate and lung cancer. Increased HDAC activity can lead to tumorigenesis, including uncontrolled cell proliferation and

apoptosis [7]. It was found that suppressing HDAC activity could lead to down-regulation of the Slug gene which is involved in epithelial to mesenchymal transition (EMT) reversal [9]. Tumor cells undergo EMT, which can lead to malignancy and metastatic spread to distant regions, reducing survival rates of patients with breast cancers. An increasing amount of evidence suggests that cancer cells can employ EMT to promote tumor growth and invasion. Tumor cells can metastasize, retain stemness, defend chemotherapy, and exhibit plasticity [10]. During tumor formation, cancer cells undergo highly dynamic changes in the expression profile of adhesion molecules, which cause the cells to detach from their native tissue and acquire an extremely motile and invasive character [11]. Epigenetic alterations, such as histone modifications also govern the process of EMT. HDAC inhibitors can influence the expression of EMT-related proteins, with their effects varying depending on the type of cancer [12]. As epigenetic and EMT changes are reversible, focusing on these tumor-suppressor genes offers a novel strategy to prevent the development and spread of cancer [7]. The malignant aspect of tumor arises from their metastatic dissemination, which is more challenging to target than the proliferation of cells [13]. The EMT process is mainly governed by PI3K/Akt pathway and regulates cell growth and malignant behaviour in cancer cells. The PI3K/Akt pathway-mediated EMT has raised concerns as a potential target for preventing and treating the metastatic tumours [14].

Emerging research suggests that certain cancer cells depend on the PI3K/Akt/mTOR pathway for survival following DNA damage. Inhibiting this signaling pathway can impede DNA repair processes and increase the effectiveness of radiotherapy and chemotherapy treatments [15]. TNBC is often treated with systemic chemotherapy due to its lack of molecular targets. However, less than 20–30% of TNBC patients achieve a pathological full response to neoadjuvant treatment. Hence to effectively manage TNBC, efforts should focus on preventative approaches and discovering adjuvant chemicals to improve therapy response without severe side effects [16]. Many patients face relapse or recurrence of cancer, and acquired drug resistance has become a major challenge that often leads to the failure of cancer therapies [15].

Natural compounds have emerged as promising candidates for cancer therapy because of their potential to simultaneously target multiple pathways [17]. More than 60% of anticancer medications are derived from natural sources, and flavonoids are emerging as a promising treatment alternative due to their diverse mechanisms of action and potential to target multiple cancer-related pathways [18]. Galangin (3, 5, 7-trihydroxyflavone) (GAL) is a flavanol discovered in *Helichrysum aureonitens* plant

shoots. Gal has been shown to have diverse anti-cancer effects on a variety of malignancies, including gastric, melanoma, ovarian, hepatocellular, and promyelocytic leukaemia [19]. Additionally, combining flavonoids for example, Silibinin with TSA or Aza significantly increases E-cadherin expression while inhibiting cell migration and invasion [5]. Although Gal and berberine have distinct anticancer mechanisms, their combined effect on tumor growth remains unknown [20]. Food and its components especially structurally diverse flavonoids can affect the genome through genetic or epigenetic differences. This knowledge will be especially crucial for the prevention of health problems and the treatment of diseases like cancer [4]. Gal has been demonstrated to inhibit cancer cell development by inducing apoptosis and suppressing proliferation. However, the specific targets of Gal-induced cytotoxicity for human breast cancer cells remain unexplored [21]. This study aims to investigate the effects of Gal and its combination with the FDA-approved HDAC inhibitor Vorinostat on various anticancer targets and the modulation of epigenetic regulators involved in reversing EMT. Additionally, in vivo studies were conducted to validate and complement the detailed in vitro findings.

Materials and methods

Chemicals, reagents, and antibodies

Dulbecco's Modified Eagle Medium (DMEM) with high glucose and fetal bovine serum (FBS) was obtained from Gibco. Galangin and Suberoylanilide Hydroxamic Acid (SAHA) were sourced from Sigma-Aldrich. MTT (3-(4,5-Dimethylthiazol-2-yl)-2,5-diphenyltetrazolium bromide) was procured from Himedia, while 5-(and-6)-chloromethyl-2',7'-dichlorofluorescein diacetate acetyl ester (CM-H₂ DCFDA) was purchased from Sigma-Aldrich. The Annexin V-FITC apoptosis detection kit was obtained from BioLegend. The HDAC inhibition and HAT activity assay kits were purchased from Epigentek. Apoptosis-specific antibodies, including PARP (CST-9542) and Cleaved Caspase-9 (CST-9580), as well as HDAC-1 (CST-34589) and HDAC-3 (CST-60538) isoform antibodies, were obtained from Cell Signaling Technology (CST). The Epithelial-Mesenchymal Transition (EMT) Antibody Sampler Kit (CST-9782), Phospho-Akt (CST-4060), and Actin (CST-4970) were also acquired from CST. mTOR (E-AB-62083) and PI3K (E-AB-16199) antibodies were sourced from Elab Sciences, while PTEN (BD Bioscience-559600) was obtained from BD Biosciences. Tubulin (sc-5274) and HRP-conjugated secondary antibodies (mouse and rabbit) were purchased from Santa Cruz Biotechnology. Stock solutions of Galangin and SAHA were prepared in DMSO (Himedia) and stored at -20 °C for further experiments.

Cell culture and maintenance of MDA-MB-231 cell line

The MDA-MB-231 cell line was obtained from the National Centre for Cell Science (NCCS), Pune (Maharashtra, India), a national repository for animal cell lines. Cells were cultured in DMEM (Cat No. 11965092, Thermo Fisher), supplemented with 10% FBS (Cat No. 10270106, Thermo Fisher) and Antibiotic-Antimycotic (Cat No. 15240096, Thermo Fisher). The culture was maintained at 37 °C in a humidified incubator with 5% CO₂.

Assessment of anti-TNBC potential of Galangin and SAHA using MTT assay

To evaluate the anti-TNBC efficacy of Galangin, SAHA, and their combination, a cell viability assay was performed using the MTT assay [22–24]. MDA-MB-231 cells were seeded at a density of 1×10^4 cells per well in a 96-well culture plate and incubated overnight for adherence. Cells were then treated with increasing concentrations of Gal (25–125 $\mu\text{M}/\text{mL}$) and SAHA (2–10 $\mu\text{M}/\text{mL}$) and incubated for 48 h. After incubation, the culture medium was discarded and replaced with 100 μL of MTT reagent (Cat No. TC191, Himedia) (3-(4,5-dimethylthiazol-2-yl)-2,5-diphenyltetrazolium bromide), followed by further incubation for 4 h at 37 °C. Subsequently, 100 μL of DMSO was added to dissolve the formazan crystals, and absorbance was measured at 570 nm using a Hidex Sense multimode plate reader. Data were expressed as drug concentration versus percentage of cell proliferation. The IC₅₀ values for Galangin and SAHA were determined by testing a range of concentrations against MDA-MB-231 cells, and calculations were performed using GraphPad Prism 5.0. To further analyse the combinatorial effects, serial dilutions of Galangin and SAHA at their IC₅₀ concentrations were prepared, and the Combination Index (CI) was calculated using the Chou-Talalay equation [25].

Cell morphology assessment

The impact of Galangin, SAHA, and their combination on MDA-MB-231 cell morphology was examined using phase-contrast microscopy. Briefly, 1×10^4 cells per well were seeded into a 96-well plate and incubated overnight in a CO₂ incubator. Further, the cells were treated with Galangin (50 $\mu\text{M}/\text{mL}$), SAHA (4 $\mu\text{M}/\text{mL}$), and a combination of Galangin (0.08 $\mu\text{M}/\text{mL}$) + SAHA (1 $\mu\text{M}/\text{mL}$). Cells were incubated for 48 h, after which morphological changes indicative of cytotoxic effects were observed under a phase-contrast microscope [22–24].

Wound healing assay

The migratory potential of Galangin, SAHA, and their combination was assessed using a scratch assay. MDA-MB-231 cells were seeded in 12-well plates and incubated

until a monolayer formed. Cells were then treated with Galangin, SAHA, and a combination. Uniform scratches were introduced using sterile tips in both treated and control groups, followed by incubation for 48 h. Phase-contrast microscopy (Zeiss) was used to capture images at 0, 24, and 48 h, and wound closure was analysed with Zen software. Migration data was plotted as wound healing distance over time for control and treated cells [22–24].

Cell invasion assay

The invasive potential of MDA-MB-231 cells was examined following treatment with Galangin, SAHA, and their combination. After incubation, cells were trypsinized, and counted using a haemocytometer, and 1×10^5 cells were seeded into the upper compartment of a trans well insert. The lower chamber contained DMEM supplemented with 10% FBS. Inserts were incubated for 24 h, allowing cell migration. Non-migratory cells in the upper chamber were removed using sterile cotton swabs, while migrated cells were fixed with 4% paraformaldehyde and stained with 1% crystal violet. Phase-contrast microscopy was used for visualization, and ImageJ software was employed for analysis [22].

Reactive oxygen species (ROS) generation

Intracellular ROS generation following Galangin, SAHA, and combination treatment was evaluated using the DCFDA assay, as previously described [23, 24]. MDA-MB-231 cells (1×10^4) were seeded in 96-well plates and treated for 48 h. After incubation, cells were washed with PBS and incubated with DCFHDA (10 μM , Sigma-Aldrich, Cat. No. D6883) for 20 min, followed by three PBS washes. ROS levels were quantified using a Hidex Sense multimode spectrophotometer, and DCF uptake was visualized using a live-cell imaging system (Zeiss Cell Discoverer 7.0) [23, 24]. The N-acetyl-L-cysteine (NAC), a known antioxidant agent, was used as a positive control during the DCFDA study.

Nuclear staining with DAPI in Galangin, SAHA, and combination-treated TNBC cells

TNBC cells (1×10^4) were seeded in 96-well plates and treated with Galangin, SAHA, or their combination for 48 h. Post-treatment, cells were washed with PBS and stained with DAPI (5 $\mu\text{g}/\text{mL}$, Invitrogen, Cat No. D1306) for 20 min. Excess stain was removed by PBS washing, and nuclear morphology was examined using a live-cell imaging system (Zeiss Cell Discoverer 7.0) [24].

Mitochondrial membrane potential assessment using JC-1 in Galangin, SAHA, and combination-treated TNBC cells

Following 48 h of treatment with Galangin, SAHA, and their combination, TNBC cells (1×10^4) were washed

with PBS and incubated with JC-1 (5 µg/mL, Thermo Fisher, Cat No. T3168) for 20 min. After a final PBS wash, mitochondrial membrane potential changes were visualized using the live-cell imaging system (Zeiss Cell Discoverer 7.0) [24].

FACS-based cell cycle analysis

To evaluate cell cycle phase distribution and its regulation post-treatment, TNBC cells (1×10^5) were seeded in 6-well plates and exposed to Galangin, SAHA, or their combination for 48 h. Cells were then stained with propidium iodide (50 µg/mL, Sigma Aldrich, Cat No. P4170) and analysed via flow cytometry. Phase distribution was assessed using BD FACSDiva™ software [23, 24].

Apoptosis assays

The apoptotic effect of Galangin, SAHA, and their combination in MDA-MB-231 cells was assessed using the Annexin-V-FITC assay via flow cytometry [23, 24]. Cells (1×10^5) were seeded in 6-well plates and treated with Galangin, SAHA, or their combination. Following treatment, cells were washed with PBS and stained with Annexin V-FITC (50 µg/mL, BioLegend, Cat No. 640906) and PI (50 µg/mL). Stained cells were analysed using a BD Bioscience flow cytometer, and apoptosis quantification was performed using BD FACSDiva™ software [23, 24].

HDAC Inhibition assay

HDAC inhibition by Galangin was evaluated using a fluorometric HDAC assay kit. After treatment, MDA-MB-231 cells were harvested, and nuclear extracts were prepared using the EpiQuik™ Nuclear Extraction Kit (Cat No. OP-0002-1). HDAC activity was measured using the Epigentek HDAC Assay Kit (Base Catalog # P-4034) per manufacturer instructions. The activity was calculated using the formula: HDAC Activity (OD/min/mg) = (Sample OD – Blank OD) / (Protein Amount (µg) × min) [24].

HAT activity assay

The regulatory effect of Galangin on HAT activity was assessed using a HAT inhibition assay. MDA-MB-231 cells were treated for 48 h, and nuclear extracts were prepared using the EpiQuik™ Nuclear Extraction Kit (Cat No. OP-0002-1). HAT activity was measured using the EpiQuik™ HAT-Activity/Inhibition Assay Kit (Cat No. P-4003). The activity was calculated as:

HAT Activity (OD/h/mg protein) = (OD untreated sample – blank) × 1000 / (h × protein amount (µg)) [24].

Quantitative expression analysis of epigenetic regulators, EMT markers, and PI3K pathway proteins via qRT-PCR

The impact of Galangin, SAHA, and their combination on the expression of epigenetic regulators, EMT markers,

and PI3K pathway components was assessed using qRT-PCR, following our previous protocol [22–24]. Total RNA from treated and control samples was extracted using TRIZOL reagent (Ambion, Cat No. 15596018), diluted in nuclease-free water, and quantified using a Nanodrop spectrophotometer (Implen). Reverse transcription was performed using the iScript cDNA synthesis kit (Bio-Rad, Cat No. 1708890) under the following conditions: 25 °C for 5 min, 46 °C for 20 min, and 95 °C for 5 min using a MyCycler Thermal Cycler (Bio-Rad). Real-time PCR was conducted with SYBR Green (Bio-Rad, Cat No. 171–5121) on a Bio-Rad CFX96 system. Target genes included HDAC isoforms, EMT markers (E-cadherin, N-cadherin, Snail, Slug, MMP-9, MMP-2, and Zeb), and PI3K pathway components (TGFβ, AKT, PI3K, mTOR, and PTEN), with GAPDH as the internal control (Table S1, Supplementary Information). Fold changes in gene expression were calculated using the $2^{-\Delta\Delta CT}$ method.

Immunoblotting analysis of epigenetic regulators, EMT markers, and PI3K pathway proteins

The protein expression levels of epigenetic regulators, EMT markers, and PI3K pathway components were evaluated via immunoblotting in treated and control MDA-MB-231 cells, following established protocols [22–24]. Cells (2×10^5) were seeded in 60 mm dishes and treated with Galangin, SAHA, or their combination for 48 h. Post-treatment, cells were washed with PBS, scraped, and lysed using RIPA buffer (Thermo Fisher, Cat No. 89900) supplemented with a protease inhibitor (HiMedia, Cat No. ML051). Protein concentrations were determined using the Bradford assay (HiMedia, Cat No. ML106). Equal amounts of total protein (50 µg) were separated by SDS-PAGE (7.5–12% gels, Bio-Rad, Cat No. 161–0377) and transferred onto PVDF membranes (Cytiva, Cat No. 10600021). Membranes were blocked with skimmed milk for 1 h, washed with TBST, and incubated overnight at 4 °C with primary monoclonal antibodies. After additional TBST washes, membranes were incubated with appropriate secondary antibodies for 1–2 h at room temperature. Protein bands were visualized using an ECL detection reagent (Advansta, Cat No. K-12045-D20) and imaged with an Amersham Gel Imager 680.

Confocal microscopy for EMT protein expression

To visualize EMT-associated protein expression, confocal microscopy was performed. MDA-MB-231 cells were cultured as a monolayer on glass coverslips in 12-well plates and treated with Galangin, SAHA, and their combination for 48 h. Post-treatment, cells were washed with PBS, fixed with 4% paraformaldehyde for 15 min, and permeabilized with 0.1% Triton X-100 for 10 min. After three PBS washes, cells were incubated overnight with primary antibodies against E-cadherin and Slug.

Following a 24-hour incubation, cells were washed thrice and probed with the corresponding secondary antibody for 1 h at room temperature. Coverslips were mounted using Abcam's mounting medium (Cat No. ab104139), and fluorescence images were acquired using a Leica SP8 confocal microscope [26].

In vivo tumor model study

The in vivo effects of Galangin, SAHA, and their combination were evaluated in BALB/c mice, following Institutional Animal Ethics Committee (IAEC) guidelines (Approval No. EAF/2023/B453, NCCS Pune, MS, India). Six-to-eight-week-old mice were injected subcutaneously with 4T1 cells (1×10^5 in 0.1 mL PBS, pH 7.2). Upon tumor palpation, mice were randomly assigned to four groups ($n=6$): Group 1 received vehicle control, Group 2 was intraperitoneally injected with Gal (25 mg/kg), Group 3 received SAHA (5 mg/kg), and Group 4 received a combination of Gal (25 mg/kg) and SAHA (5 mg/kg). Mice were monitored for 20 days, with tumor volume and body weight measured every four days. On day 21, final weights were recorded, and mice were sacrificed for tumor excision. Tumor volume (V) was calculated using the formula: $V = L \times W^2 \times 0.52$ (L=length, W=width). Excised tumours were processed for histopathological analysis via haematoxylin and eosin (H&E) staining [27].

Statistical analysis

All experiments were performed in triplicate. Data were analysed using one-way ANOVA in GraphPad Prism (version 5.01). Results are expressed as mean \pm SD from three independent replicates. Statistical significance is denoted as $p < 0.05$ (*), $p < 0.01$ (**), and $p < 0.001$ (***)

Results

Effect of Galangin, SAHA, and their combination on MDA-MB-231 cell viability

The anti-TNBC potential of Galangin, SAHA, and their combination on MDA-MB-231 cells was evaluated using the MTT assay. A dose-dependent decrease in cell viability was observed after 48 h of treatment (Fig. 1A). At its IC_{50} concentration (50 μ M/mL), Galangin induced 50% cell death in MDA-MB-231 cells, while viability further declined to 10% at 125 μ M/mL. In contrast, MDA-MB-231 cells exhibited greater sensitivity to SAHA, showing 50% cell death at an IC_{50} of 4 μ M/mL and a reduction in viability to 15% at 10 μ M/mL (Fig. 1B). A synergistic cytotoxic effect was observed when Galangin and SAHA were combined, significantly reducing MDA-MB-231 cell viability at IC_{50} concentrations of 0.08 μ M/mL for SAHA and 1 μ M/mL for Galangin (Fig. 1C). Additionally, treatment with Galangin, SAHA, and their combination induced adverse morphological changes in TNBC cells. The cells were rounded, detached from the substratum, and floated in the culture medium, indicating a loss of adherence and viability (Fig. 1E and G).

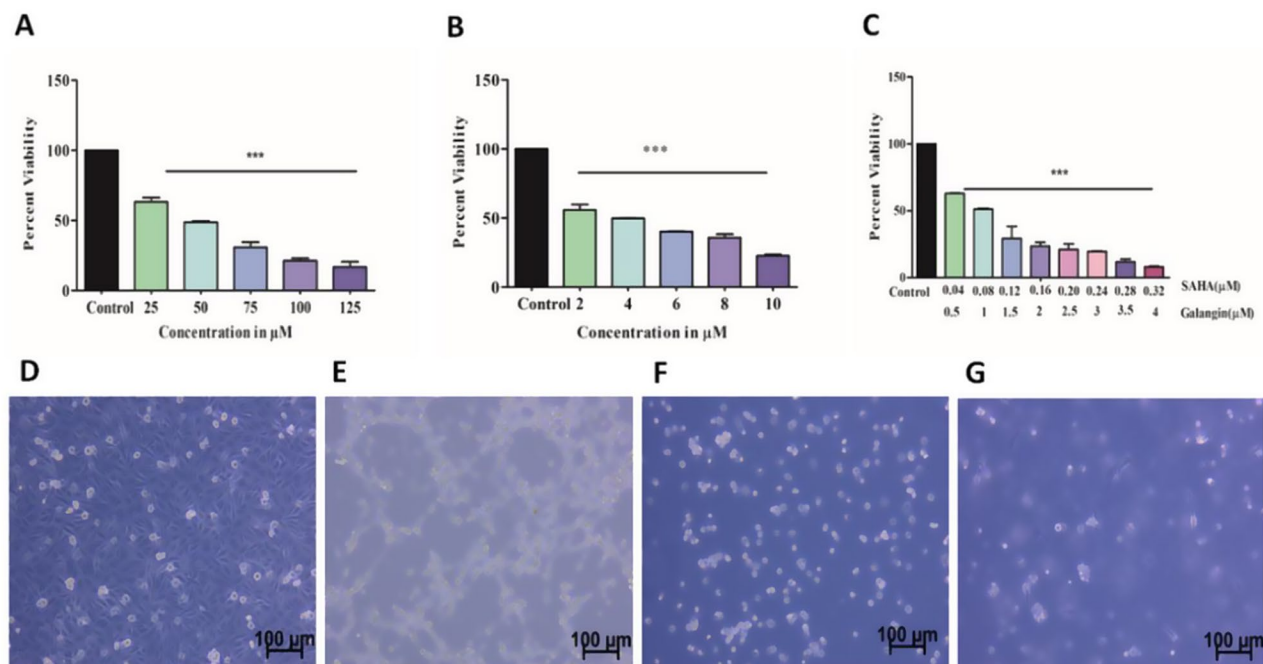


Fig. 1 Impact of (A) Galangin, (B) SAHA, and (C) their combination on the viability of MDA-MB-231 cells. Morphological assessment of MDA-MB-231 cells: (D) Untreated control cells displaying normal morphology, (E) Galangin-induced morphological alterations, (F) SAHA-induced changes, and (G) Morphological effects resulting from the combined treatment with Galangin and SAHA

Galangin, SAHA, and their combination inhibit migration and invasion of MDA-MB-231 cells

The anti-metastatic and anti-invasive effects of Galangin, SAHA, and their combination on MDA-MB-231 cells were evaluated using wound healing and trans well assays (Fig. 2).

Treatment with Galangin, SAHA, and their combination reduced TNBC cell migration by approximately 50%, 80%, and 90%, respectively, compared to control cells after 24 h (Fig. 2A and C). Notably, the combination

treatment exhibited the most significant inhibition of migration after 48 h. Furthermore, Galangin, SAHA, and their combination suppressed the invasive capacity of TNBC cells by 60%, 50%, and 80%, respectively, compared to control cells after 48 h (Fig. 2B and D). Both Galangin alone and in combination with SAHA effectively inhibited cell migration, invasion, and metastatic potential in MDA-MB-231 cells. These findings suggest that Galangin exerts anti-metastatic effects similar to SAHA and may serve as a complementary anticancer

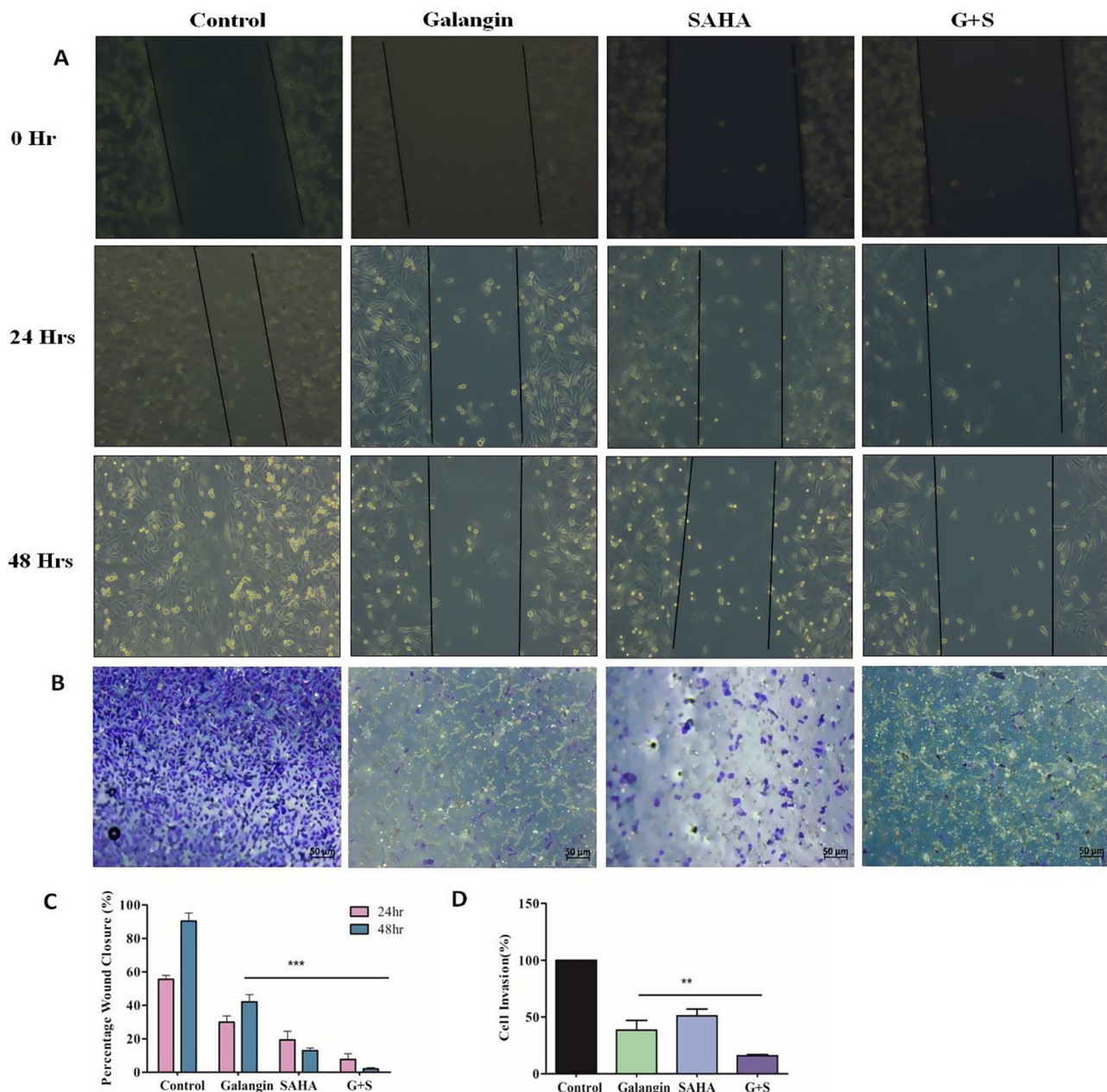


Fig. 2 (A) Inhibition of MDA-MB-231 cell migration by Galangin, SAHA, and their combination following 24 and 48 h of treatment, (B) Suppression of MDA-MB-231 cell invasion upon treatment with Galangin, SAHA, and their combination, (C) Quantification of wound closure percentage post-treatment with Galangin, SAHA, and their combination, and (D) Measurement of cell invasion percentage after exposure to Galangin, SAHA, and their combination

agent by reducing the invasiveness and metastatic potential of MDA-MB-231 cells.

Galangin, SAHA, and Their Combination Induce Reactive Oxygen Species (ROS) Generation and Reduce Mitochondrial Membrane Potential ($\Delta\Psi$ M) in MDA-MB-231 Cells.

The generation of intracellular reactive oxygen species (ROS) in MDA-MB-231 cells following treatment with Galangin, SAHA, and their combination was assessed using DCFDA staining. The uptake of DCFDA by control and treated cells was analysed through a colorimetric method and live-cell imaging (Fig. 3A). High fluorescence intensity in treated cells correlated with elevated ROS levels, leading to increased cell death (Fig. 3A and D). Greater DCFDA uptake was associated with enhanced cytotoxicity, likely due to the heightened sensitivity of MDA-MB-231 cells to Galangin and SAHA. ROS generation significantly increased after the treatment with Galangin, SAHA, and their combination. The synergistic effect of both compounds further amplified cell death in TNBC cells. Elevated ROS levels are prone to induce oxidative stress, triggering apoptotic-mediated cell death. These findings were validated using NAC, a well-known antioxidant, as a positive control. NAC-pretreated cells exhibited reduced ROS generation and subsequently reduced cell death upon exposure to Galangin, SAHA, or their combination (Fig. 3E and digitised images in supplementary file).

This confirms the role of Galangin, alone and in combination with SAHA in ROS-mediated cytotoxicity in MDA-MB-231 cells. Likewise, DAPI uptake was observed in MDA-MB-231 cells following treatment with Galangin, SAHA, and their combination (Fig. 3B). DAPI intercalates into the DNA of dead cells, with increased DAPI-stained nuclei indicating higher levels of cell death. In this study, nuclear fragmentation, chromatin condensation, and reduced cell division were evident in treated MDA-MB-231 cells compared to controls (Fig. 3B), confirming that Galangin and its combination with SAHA effectively induce apoptotic-mediated cell death in TNBC cells. Additionally, a significant reduction in mitochondrial membrane potential ($\Delta\Psi$ M) was observed in TNBC cells treated with Galangin, SAHA, and their combination (Fig. 3C). The fluorescent dye 5,5,6,6'-tetrachloro-1,1',3,3'-tetraethylbenzimidazoly-lcarbocyanine iodide (JC-1) was used to detect $\Delta\Psi$ M in both healthy and treated MDA-MB-231 cells. JC-1 is a lipophilic, cationic dye that accumulates in mitochondria, forming concentration-dependent J-aggregates, which exhibit red fluorescence (~590 nm). In healthy TNBC cells with intact $\Delta\Psi$ M, JC-1 accumulates in mitochondria, forming red fluorescent J-aggregates, as shown in Fig. 3C. However,

in MDA-MB-231 cells treated with Galangin, SAHA, or their combination, increased membrane permeability led to a loss of mitochondrial electrochemical potential, preventing J-aggregate formation. As a result, JC-1 retained its original green fluorescence (Fig. 3C and F). Elevated green fluorescence signifies apoptotic-mediated cell death in treated TNBC cells. These findings align with DCFDA and DAPI results, further supporting that Galangin and its combination with SAHA induce apoptosis in TNBC cells, comparable to the reference drug SAHA.

Galangin, SAHA, and their combination induce cell cycle arrest and Apoptotic-Mediated cell death in MDA-MB-231 cells

Flow cytometry analysis using propidium iodide staining was conducted to investigate the effects of Galangin, SAHA, and their combination on cell cycle regulation in MDA-MB-231 cells (Fig. 4). In control cells, approximately 70% and 10% of the population were in the G1 and S phases, respectively, indicating normal cell cycle progression (Fig. 4A). In contrast, Galangin and SAHA treatment led to 80–90% of cells being arrested in the SubG0/G1 phase (Fig. 4B and C). A similar trend was observed in the combinatorial treatment, where approximately 85% of cells were arrested in the SubG0/G1 phase (Fig. 4D). These findings highlight the synergistic effect of Galangin and SAHA in disrupting cell cycle progression in cancer, suggesting that Galangin exerts its effects through a mechanism similar to SAHA.

Further, Annexin V-FITC flow cytometry was performed to assess apoptotic-mediated cell death following treatment with Galangin, SAHA, and their combination (Figs. 4F–J). In control cells, 64.4% remained viable, while only 9.4% exhibited apoptosis (Fig. 4F). In contrast, Galangin treatment reduced viability to 44.6%, with apoptotic-mediated cell death increasing to 31.6% (Fig. 4G). SAHA-treated cells displayed even higher apoptosis, with 52.7% of cells undergoing apoptotic-mediated cell death and only 5.6% remaining viable (Fig. 4H). The combination treatment resulted in 63.1% apoptotic-mediated cell death, leaving only 5% of cells viable (Fig. 4I). Notably, combinatorial treatment exhibited a higher apoptotic population and lower necrotic population compared to SAHA alone, underscoring the enhanced synergistic role of Galangin and SAHA in inducing apoptosis in MDA-MB-231 cells. Apoptotic-mediated cell death in MDA-MB-231 cells following Galangin, SAHA, and combination treatment might be driven by ROS generation, nuclear fragmentation, chromatin condensation, mitochondrial membrane potential reduction, and cell cycle arrest at the Sub G0/G1 phase.

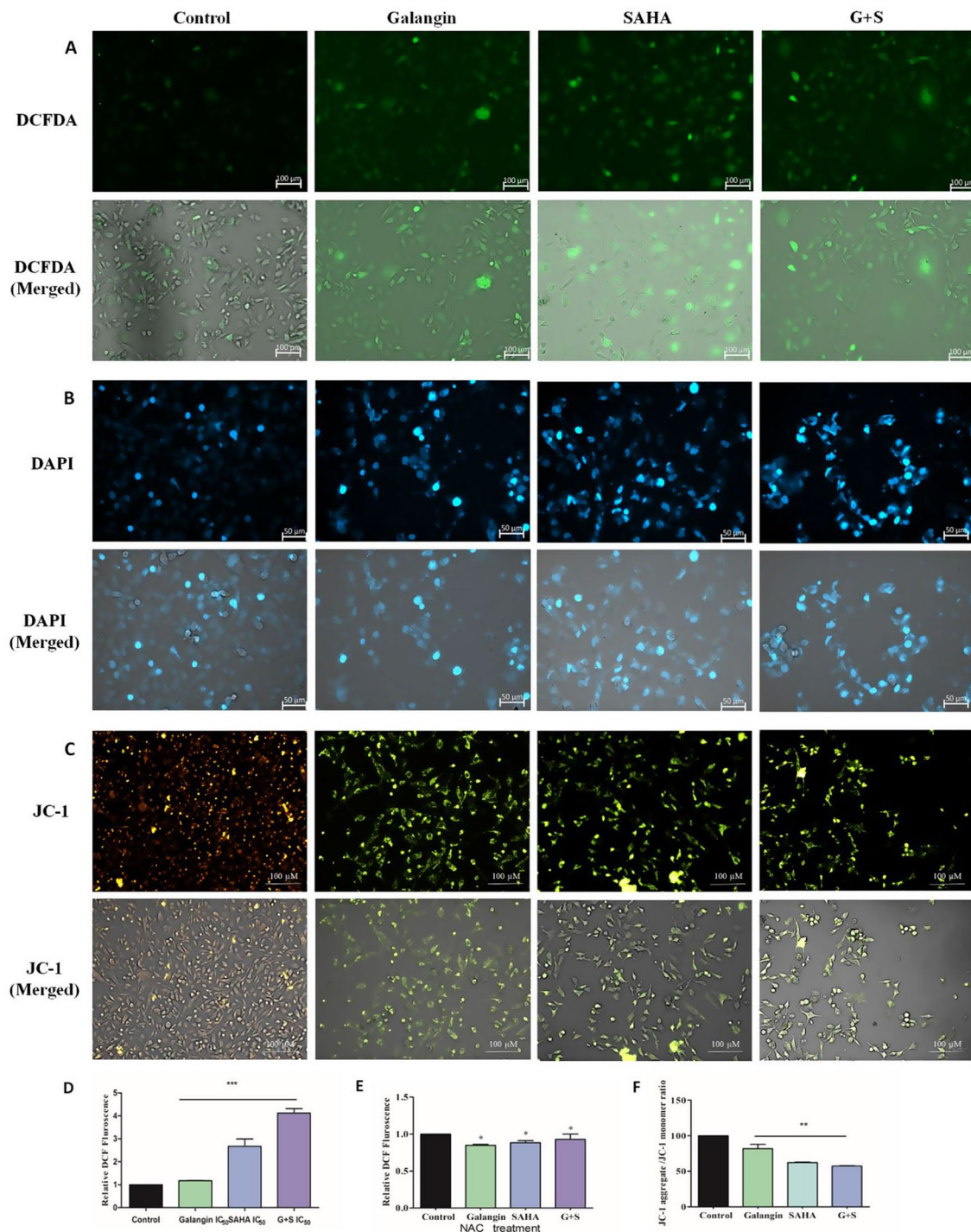


Fig. 3 Impact of Galangin, SAHA, and their combination on (A) ROS production in MDA-MB-231 cells, (B) Apoptotic morphological changes, (C) Mitochondrial membrane potential, (D) Relative DCF fluorescence, and (E) Relative DCF fluorescence after NAC pretreatment, and (F) Statistical analysis of $\Delta\Psi_m$ reduction

Galangin inhibits HDAC activity and enhances HAT activity in MDA-MB-231 cells

The HDAC inhibitory potential of Galangin was evaluated using an enzymatic assay kit. Results indicated a dose-dependent increase in HDAC inhibition in

MDA-MB-231 cells treated with Galangin (Fig. 5A). At its IC₅₀ concentration, Galangin inhibited HDAC activity by approximately 50%, while inhibition increased to 82% at the IC₇₅ concentration. Notably, HDAC inhibition at the IC₇₅ concentration was nearly equivalent to

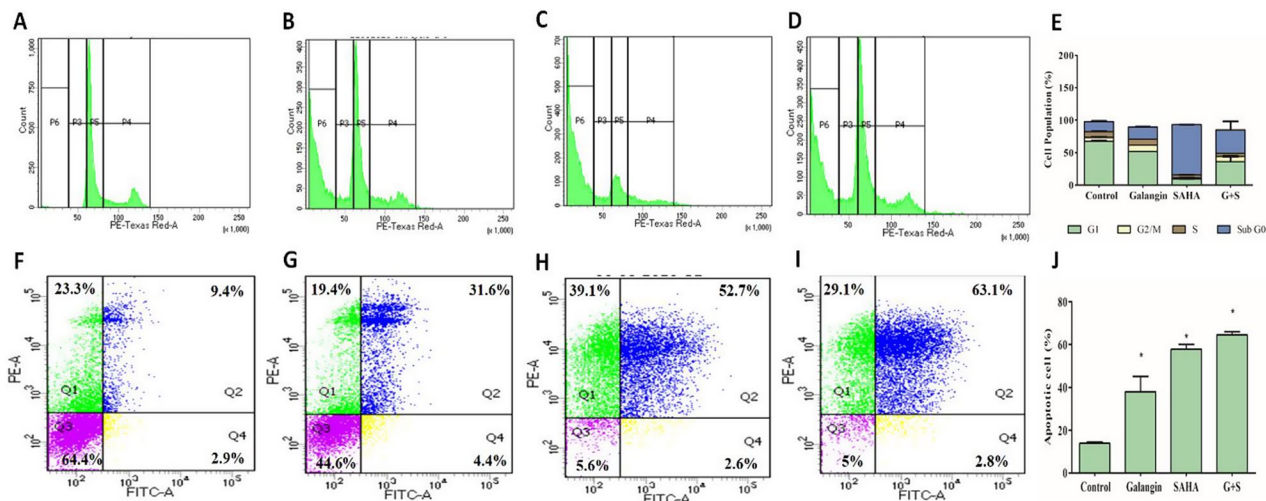


Fig. 4 (A) Untreated MDA-MB-231 control cells, (B) Cells exposed to Galangin, (C) Cells treated with SAHA, and (D) Cells subjected to the combined treatment of Galangin and SAHA, (E) Percent distribution of cell populations across different cell cycle phases, (F) Control cells with a predominant live cell population. Apoptotic-mediated cell death induced by (G) Galangin, (H) SAHA, and (I) Galangin and SAHA combination, (J) Quantified apoptotic-mediated cell death in MDA-MB-231 cells, categorized as Q1: Necrotic, Q2: Apoptotic, Q3: Live, and Q4: Early apoptotic cells

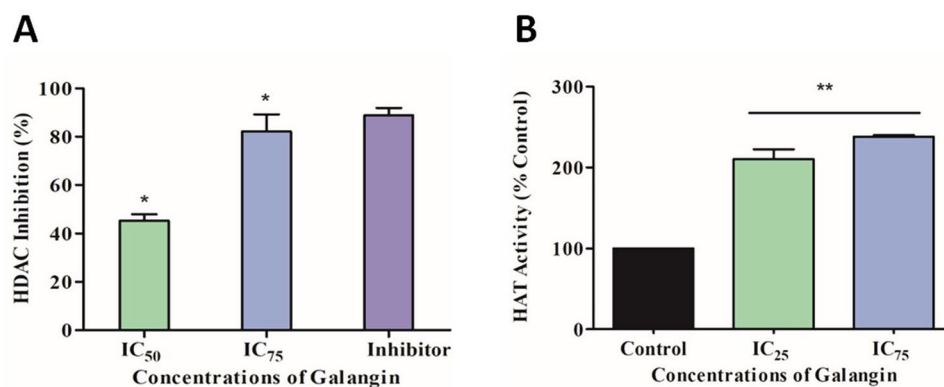


Fig. 5 (A) Dose-dependent inhibition of HDAC activity by Galangin, and (B) Dose-dependent increase in HAT activity by Galangin in MDA-MB-231 cells

that of the standard HDAC inhibitor provided in the assay kit (Fig. 5A). Conversely, a dose-dependent rise in HAT activity was observed following Galangin treatment (Fig. 5B). Compared to control cells, HAT activity nearly doubled at IC₅₀ and IC₇₅ concentrations of Galangin. The balance between HDAC and HAT activity is crucial for normal cellular regulation, whereas its disruption is a hallmark of cancer. The observed reduction in HDAC activity and concurrent increase in HAT activity at IC₅₀ and IC₇₅ concentrations suggest that Galangin modulates epigenetic regulators, restoring normal cell function and inhibiting cancer cell proliferation.

Galangin, SAHA, and their combination modulate epigenetic regulators, EMT markers, and PI3K pathway markers in MDA-MB-231 cells: analysis using qRT-PCR

The effects of Galangin, SAHA, and their combination on the expression of epigenetic regulators (HDAC isoforms), EMT markers, and key proteins in the PI3K/AKT/mTOR

pathway were analysed using qRT-PCR (Fig. 6). Treatment with Galangin resulted in the downregulation of HDAC isoforms 1–10, while HDAC11 was upregulated (Fig. 6A). Notably, HDAC1–5 and HDAC10 showed significant downregulation. In contrast, SAHA-treated MDA-MB-231 cells exhibited downregulation of all HDAC isoforms except HDAC2 (Fig. 6B). Interestingly, combinatorial treatment with Galangin and SAHA led to the downregulation of all HDAC isoforms (Fig. 6C). This suggests that the combination treatment exerts a stronger synergistic effect compared to individual treatments with Galangin or SAHA alone. Galangin, SAHA, and their combination also influenced the expression of epithelial and mesenchymal markers (Fig. 6D and F). Galangin treatment upregulated the epithelial marker E-cadherin while significantly downregulating mesenchymal markers, including N-cadherin, Snail, Slug, Zeb, MMP-2, and MMP-9 (Fig. 6D).

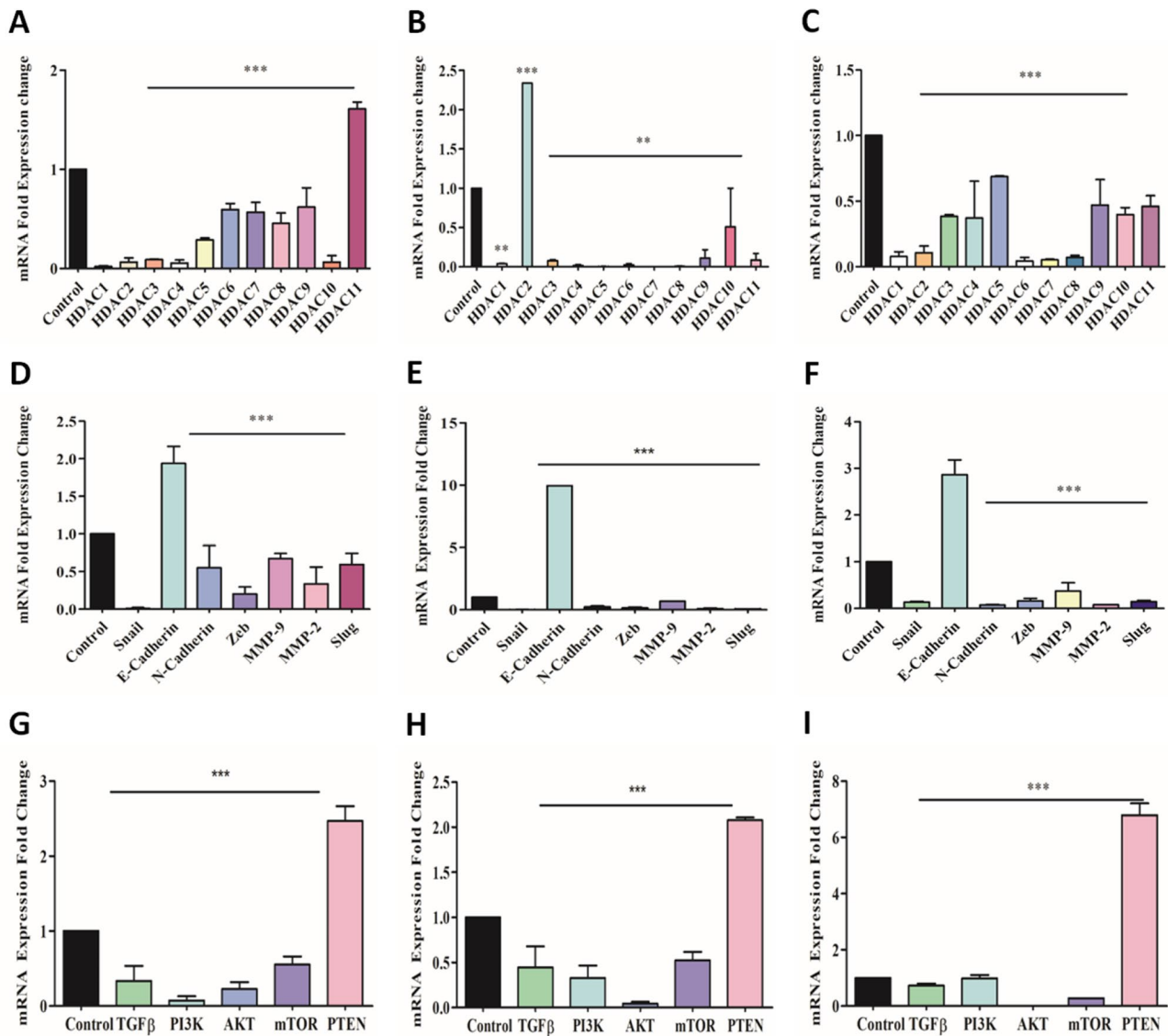


Fig. 6 Regulation of epigenetic modulators (HDAC isoforms) by (A) Galangin, (B) SAHA, and (C) Combination of Galangin and SAHA. Expression changes in epithelial and mesenchymal markers induced by (D) Galangin, (E) SAHA, and (F) A combination of Galangin and SAHA. Modulation of key proteins in the PI3K/AKT/mTOR pathway by (G) Galangin, (H) SAHA, and (I) Combination of Galangin and SAHA

SAHA exhibited a more pronounced effect, markedly reducing the expression of mesenchymal markers and increasing E-cadherin expression (Fig. 6E). The combinatorial treatment also upregulating E-cadherin and downregulating mesenchymal markers at levels comparable to SAHA (Fig. 6F). These findings indicate that Galangin and SAHA, both individually and in combination, reverse the EMT process, restore epithelial characteristics, and suppress metastatic potential by modulating mesenchymal and epithelial marker expression.

Given the established role of the PI3K/AKT/mTOR pathway in cancer initiation, proliferation, metastasis, and angiogenesis, we explored its correlation with epigenetic regulators and EMT markers in MDA-MB-231

cells (Fig. 6G and I). Galangin, SAHA, and their combination downregulated oncogenic proteins such as TGFβ, PI3K, AKT, and mTOR while upregulating the tumor suppressor protein PTEN. These findings align with the expression profiles of epigenetic regulators and EMT markers, suggesting a potential link between these molecular pathways. The downregulation of HDACs may contribute to the suppression of mesenchymal markers and oncogenic proteins, while the concurrent upregulation of HAT, epithelial markers, and tumor suppressor proteins facilitates EMT reversal, thereby inhibiting invasion and metastasis in MDA-MB-231 cells.

Galangin, SAHA, and their combination modulate epigenetic regulators, EMT markers, and PI3K pathway markers in MDA-MB-231 cells: validation using Immunoblotting analysis

The effects of Galangin, SAHA, and their combination

on epigenetic regulators, EMT markers, pro-apoptotic markers, and the PI3K pathway were examined at the proteomic level using immunoblotting analysis (Fig. 7). Treatment with Galangin, SAHA, and their combination reduced the expression of HDAC1 and HDAC3 by

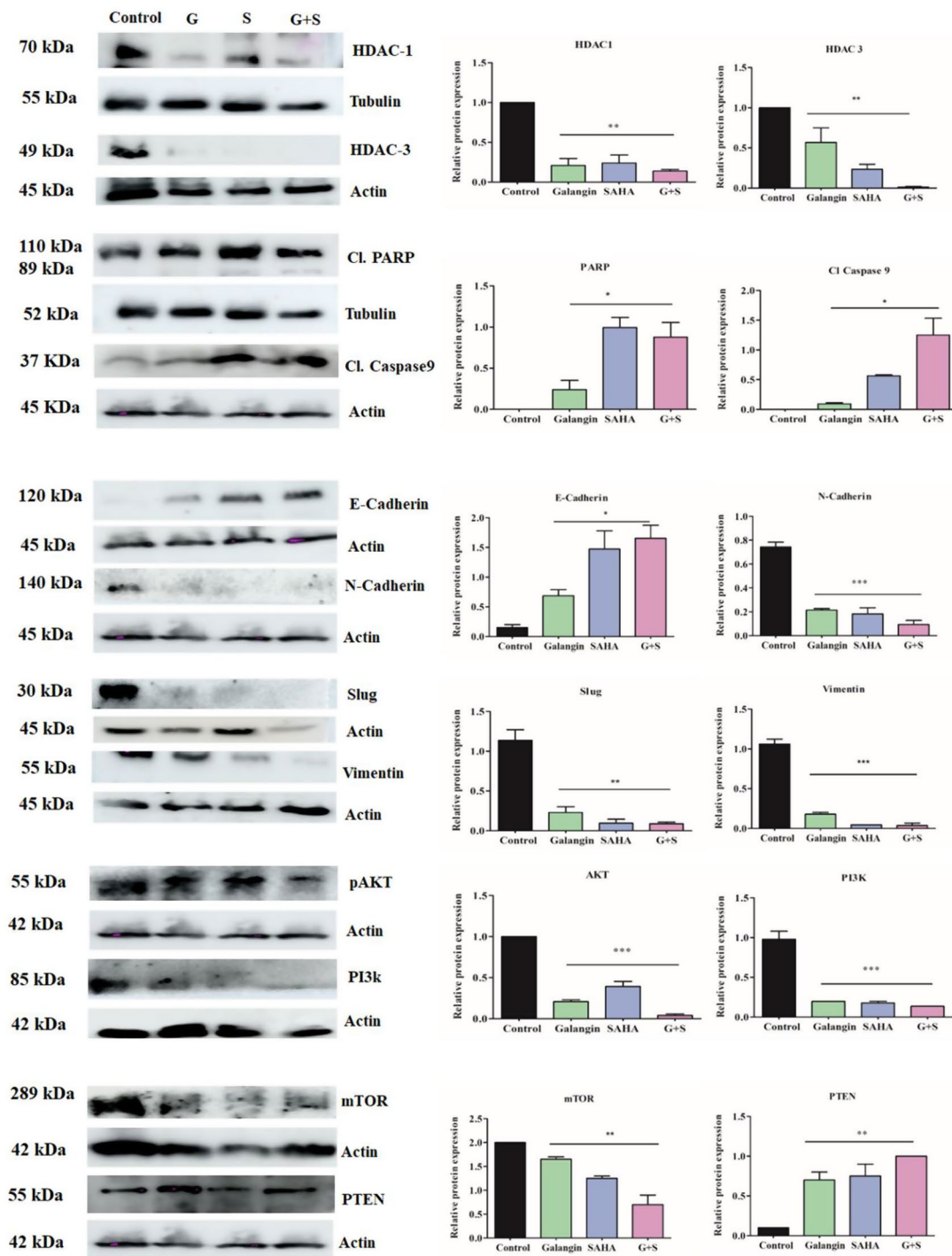


Fig. 7 Immunoblot analysis illustrating the impact of Galangin, SAHA, and their combination on the expression of epigenetic regulators (HDAC1, HDAC3), pro-apoptotic proteins (PARP, Caspase-9), EMT markers (E-cadherin, N-cadherin, Snail, Slug), PI3K/AKT/mTOR pathway proteins, and the tumor suppressor PTEN in MDA-MB-231 cells

0.7/0.5, 0.7/0.7, and 0.8/0.9-fold, respectively, compared to untreated MDA-MB-231 cells (Fig. 7). Galangin primarily downregulated HDAC1, while SAHA exhibited a stronger effect on HDAC3. The combinatorial treatment significantly suppressed both HDAC1 and HDAC3, reinforcing the synergistic effect of Galangin and SAHA. In contrast, the cleaved pro-apoptotic markers PARP and Caspase-9 increased by 0.3/0.1, 1.0/0.6, and 0.9/0.9-fold following individual and combinatorial treatment with Galangin and SAHA. This suggests enhanced apoptosis in response to these treatments.

Further, Galangin, SAHA, and their combination upregulated E-cadherin expression by 0.6, 1.5, and 1.7-fold, respectively, compared to control cells (Fig. 7). Conversely, mesenchymal markers such as N-cadherin, Slug, and Vimentin were sequentially downregulated in response to Galangin, SAHA, and their combination, further supporting the role of these compounds in reversing the EMT process. Treatment with Galangin, SAHA, and their combination led to a significant reduction in the expression of oncogenic proteins PI3K, AKT, and mTOR by 0.7/0.7/0.2, 0.7/0.6/0.4, and 0.8/0.9/0.7-fold, respectively, compared to control cells (Fig. 7). Meanwhile, tumor suppressor PTEN expression was increased by 0.6, 0.7, and 0.9-fold following treatment with Galangin, SAHA, and their combination, further confirming their role in suppressing tumorigenic pathways in MDA-MB-231 cells. These findings highlight the effectiveness of Galangin, both alone and in combination with SAHA, in modulating key regulatory proteins involved in epigenetics, apoptosis, EMT, and the PI3K/AKT/mTOR

pathway, contributing to its potential as an anti-cancer agent.

Similarly, treatment with Galangin, SAHA, and their combination led to the downregulation of epigenetic regulators, mesenchymal markers, and oncogenic proteins, while upregulating epithelial markers, pro-apoptotic markers, and the tumor suppressor protein. The proteomic findings align with transcriptomic data, further confirming that Galangin, SAHA, and their combination induce apoptotic-mediated cell death in MDA-MB-231 cells.

Galangin, SAHA, and their combination reverse EMT by modulating E-Cadherin and slug expression in MDA-MB-231 cells: an Immunofluorescence study

To validate the qRT-PCR and immunoblotting findings, immunofluorescence analysis was performed using confocal microscopy to examine the expression of epithelial and mesenchymal markers (Fig. 8). In control cells, the epithelial marker E-cadherin (green fluorescence) showed low expression (Fig. 8). Whereas treatment with Galangin, SAHA, and their combination significantly increased E-cadherin levels. Conversely, the mesenchymal marker Slug was highly expressed in control cells but markedly reduced following Galangin, SAHA, and combination treatments. These results suggest that Galangin and SAHA help maintain the epithelial phenotype of MDA-MB-231 cells by suppressing mesenchymal traits, as evidenced by E-cadherin upregulation and Slug downregulation in both individual and combinatorial treatments. Furthermore, these findings reinforce the role of

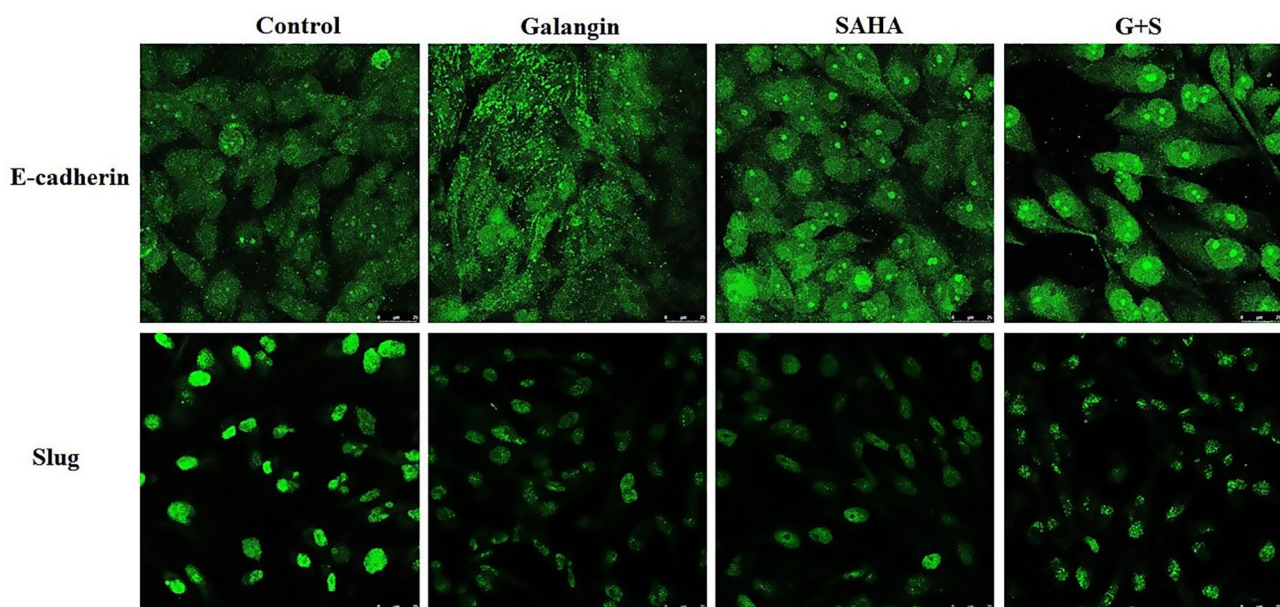


Fig. 8 Effect of Galangin, SAHA, and their combination on EMT regulator expression, specifically E-cadherin and Slug, in control and treated MDA-MB-231 cells

Galangin, SAHA, and their combination in EMT reversal in MDA-MB-231 cells.

In vivo validation of the Anti-TNBC potential of Galangin, SAHA, and their combination using a BALB/c mice model and histopathology analysis

The anti-TNBC efficacy of Galangin, SAHA, and their combination was validated through an in vivo study using a BALB/c mice model. Tumor size and body weight were measured on every four days by using Vernier callipers (Fig. 9A and D). On day 21, mice were sacrificed in CO₂ chambers, and tumours were excised for further analysis (Fig. 9B and D). Tumor size was significantly reduced following treatment with Galangin, SAHA, and their combination compared to control tumours, with the greatest reduction observed in the combination group, indicating a synergistic effect. Additionally, tumor volume and body weight were markedly lower in treated mice compared to controls (Fig. 9C and D), supporting the anti-TNBC potential of Galangin and SAHA. Histopathological analysis was performed to assess intra tumoral treatment efficacy using haematoxylin and eosin (H&E) staining (Fig. 9E and H). Tumours from the Galangin, SAHA, and combination-treated groups exhibited lower mitotic and necrotic scores compared to control tumours. Notably, treated tumours displayed distinct cell shrinkage and reduced tumor distribution, further supporting the anti-tumor effects of Galangin and SAHA. The BALB/c animal model and immunohistology studies reinforce the anti-tumor efficacy of Galangin, SAHA, and their combination, demonstrating their potential in TNBC treatment.

Discussion

Triple-negative breast cancer (TNBC) is aggressive, heterogeneous, and challenging to treat [1, 28]. Epigenetic dysregulation, driven by aberrant gene expression, plays a key role in cancer progression [6, 29, 30]. Epigenetic regulators like HDACs and HATs alter tumor suppressors and oncogenes, complicating treatment [29, 30]. TNBC patients face poor prognoses and frequent drug resistance, underscoring the need for targeted therapies [31]. With no effective personalized treatments, chemotherapy remains the primary option [1, 32, 33]. Researchers are exploring plant flavonoids, alone or with anticancer drugs, as alternative therapeutic approaches [34–39]. Environmental factors, such as diet, and life style also influence the epigenome, and modulate gene expression pattern [4, 4041]. The plant origin polyphenols are known to target cancer pathways, for example the dietary flavonoids like genistein from soybean and apigenin from variety of fruits, vegetables, and herb have reported to regulate the epigenetic markers in TNBC [24, 42–46]. While Galangin has been studied in various

cancer pathways, however its mechanistic role in epigenetic regulation, EMT, and PI3K/AKT/mTOR signalling in TNBC remains unclear [47, 48]. This study investigates the effects of Galangin on epigenetic regulators, EMT markers, and key signalling proteins in MDA-MB-231 cells.

Galangin exhibits strong anti-breast cancer activity, inducing morphological changes in MDA-MB-231 cells both alone and significantly in combination with SAHA. Treated TNBC cells appeared floating, irregular, and rounded, similar findings has been observed with Apigenin and SAHA [24]. Additionally, the flavanols like Fisetin and Kaempferol reduced TNBC cell growth [49, 50]. Cell migration, closely linked to metastasis, was impeded by Galangin, SAHA, and their combination, consistent with previous studies on Liquiritigenin, Cinobufagin, Quercetin, Galangin-TRAIL, and Luteolin-Curcumin combinations [21, 24, 35, 51–53]. Likewise, Baicalin also inhibited migration and invasion in colorectal cancer [54]. Galangin and SAHA induced ROS in MDA-MB-231 cells, mirroring ROS generation by Galangin in gastric cancer, Eriocitrin in lung cancer, Apigenin in TNBC, and Fisetin-Kaempferol in breast cancer [24, 37, 50, 55]. Whereas, the ROS generation was not observed in NAC-pre-treated MDA-MB-231 cells owing to antioxidant effect of NAC, these results are comparable to the earlier studies of Sulforaphane on PaCa-2 and PANC-1 cells [56].

Nuclear fragmentation, chromatin condensation, and DNA damage was observed in TNBC cells following Galangin and SAHA exposure. In line with prior studies, Galangin and SAHA arrested cell growth at the sub G0/G1 phase, while Galangin-berberine halted the cell cycle at G2/M in oesophageal carcinoma [20, 23, 24]. Furthermore, Galangin and SAHA triggered apoptosis in TNBC cells, comparable to Galangin in breast and oesophageal cancers, Apigenin-Icarin in TNBC, Baicalin-Sacubitrilat in colorectal cancer, and *Prosopis juliflora* phytochemicals in melanoma and breast cancer [20–24, 27, 34, 54]. Additionally, a crude extract of *Ruellia tuberosa* L. flower generated ROS production, promoted DNA damage and induced apoptosis in TNBC cells [57].

Recent studies have highlighted the role of dietary flavonoids in cancer prevention and metastasis inhibition through genetic and epigenetic modifications [2, 4–8, 24, 46, 48]. Similarly, Galangin and SAHA modulated epigenetic regulators by inhibiting HDAC isomers in MDA-MB-231 cells. The plant-derived compound trans-resveratrol, found in peanuts, red wine, grapes, and blueberries, demonstrated potent anti-HDAC activity [8]. Curcumin reduced p300, HDAC1, and HDAC3 levels in acute leukaemia, while Genistein increased HAT activity and induced apoptosis in prostate cancer cells [4, 6]. Likewise, Galangin and SAHA decreased HDAC

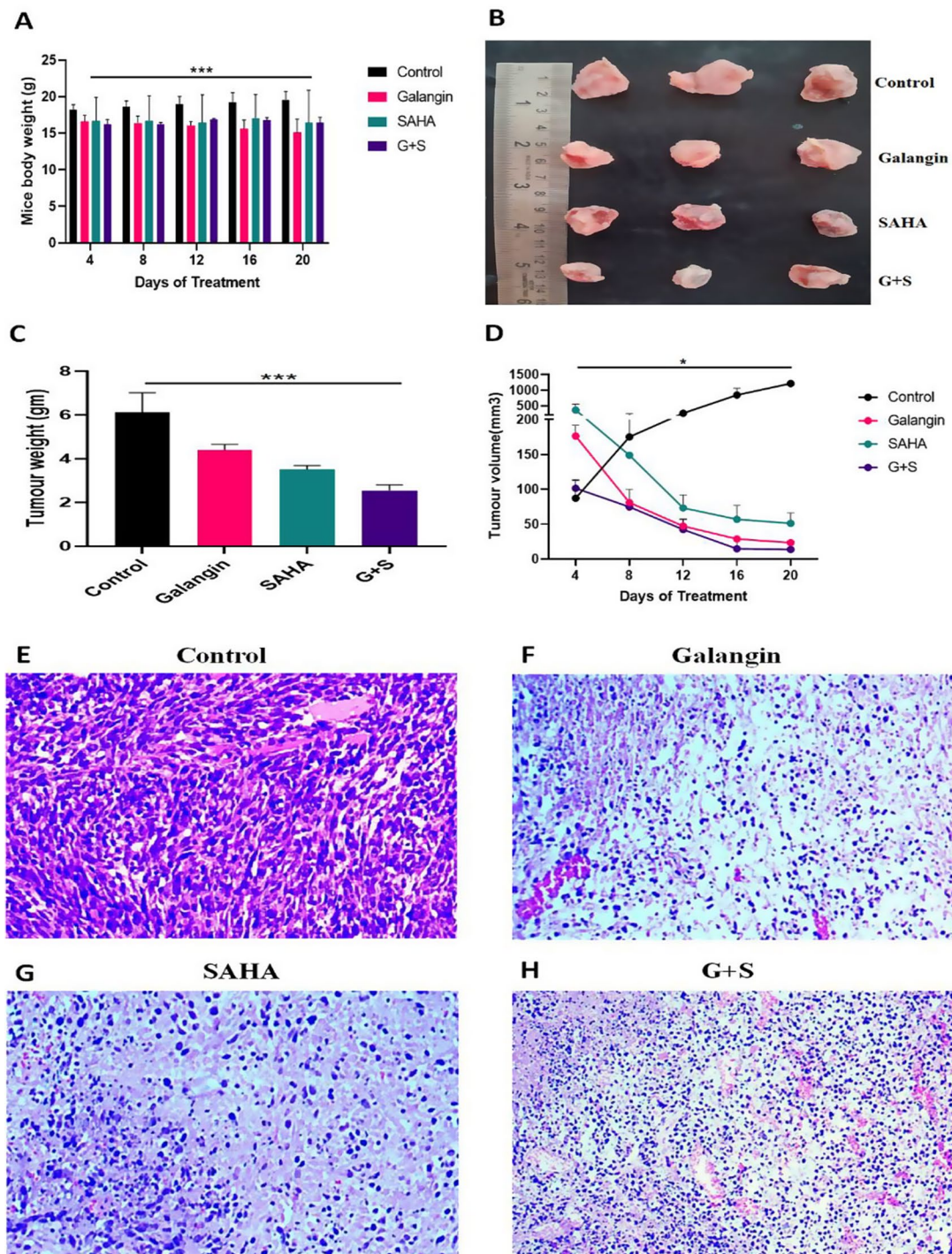


Fig. 9 (A) Effects of Galangin, SAHA, and their combination on (A) Mice body weight, (B) Tumor size, (C) Tumor weight, and (D) Tumor volume. The *p-values significantly different from the control group (* $p < 0.05$). Histological analysis of tumours: (E) PBS-treated control group exhibits moderate pleomorphism with round to oval nuclei, pink cytoplasm, and severe anaplasia. Tumours treated with (F) Galangin, (G) SAHA, and (H) their combination (G+S) show mild pleomorphism with round to oval nuclei, pink cytoplasm, and mild anaplasia

activity and increased HAT activity in a dose-dependent manner at IC_{50} and IC_{75} concentrations. Additionally, Galangin and SAHA modulated EMT markers and PI3K/AKT/mTOR pathway proteins in MDA-MB-231

cells consistent with previous findings [37–39, 51, 54, 58]. For example, Kaempferol and Cardamonin inhibited migration, invasion, and EMT by upregulating E-cadherin and downregulating N-cadherin, MMP-2,

and MMP-9 in TNBC and colon cancer cells [37, 49]. EMT is also influenced by cytokines, extracellular matrix components, TGF- β , fibroblast growth factor, epidermal growth factor, Notch pathways, and mechanotransduction [14]. Liquiritigenin, a flavonoid from *Glycyrrhiza* species increased E-cadherin and decreased N-cadherin and Vimentin in breast and colorectal cancer [51]. Immunofluorescence studies confirmed transcriptomic and proteomic results, showing reduced mesenchymal protein expression, and increased epithelial marker levels. Galangin and SAHA also downregulated PI3K, pAKT, and mTOR while increasing tumour suppressor PTEN protein expression. Transcriptomic and proteomic analyses suggest that Galangin and SAHA inhibit proliferation, migration, and invasion by generating ROS, reducing membrane potential, arresting the cell cycle at subG0/G1, and inducing apoptosis in MDA-MB-231 cells. These findings offer a promising strategy for developing effective anticancer therapies with reduced side effects.

Conclusion

The current study was intended to investigate an anti-TNBC potential of Galangin against MDA-MB-231 cells. To address the barriers presented by the rise in resistance to drugs and the off-target toxicities of traditional pharmaceuticals, active modulators must be used as a result, we have investigated how dietary flavonoid Galangin affects TNBC cells. By performing series of in vitro cell culture assays, we have demonstrated that Galangin is significantly effective in suppression of cell proliferation and reversal of EMT by blocking the PI3K/AKT pathway. Galangin at an IC₅₀ concentration of 50 μ M/mL and SAHA at 4 μ M/mL, exhibited strong anti-TNBC action by inducing adverse morphological alterations in MDA-MB-231 cells. ROS have been produced in large quantities by Galangin, which has also decreased mitochondrial membrane potential and halted the cell cycle at subG0/G1 stages. Galangin induced apoptosis-mediated cell death in TNBC cells. It downregulates HDAC and increases HAT activity, which dramatically altered the expression profile of epigenetic regulators. By upregulating the pro-apoptotic markers like Cleaved Caspase-9 and PARP proteins in TNBC cells, Galangin has induced apoptotic-mediated cell deaths in MDA-MB-231 cells. The expression of mesenchymal markers N-cadherin, Snail, Slug, Twist, Zeb, Vimentin, MMP-2, and MMP-9 was significantly downregulated by Galangin, while the expression of the epithelial marker E-Cadherin was upregulated, restoring the reversal of EMT phenomena. Following treatment of Galangin, there was a notable decrease in the PI3K/AKT/mTOR proliferation pathway and an increase in PTEN expression. Galangin and SAHA in combination synergistically suppressed MDA-MB-231 cell growth and other aspects of

TNBC progression. These outcomes are consistent with SAHA, a common HDAC inhibitor. Based on both in vitro experimental outcomes and in vivo results, it can be concluded that Galangin and SAHA might operate in a similar manner against TNBC cells. This research could contribute towards the development of a combinatorial alternative therapeutic modality for the effective management of TNBC's especially under severe and metastatic situations. Use of multiple cell lines of TNBC, detailed mechanistic studies utilizing loss-of-function and gain-of-function approaches, assessment of tumor microenvironment related studies, dose dependency and toxicity analysis, and analysis of potential off-target side effects might enrich our understanding towards exploring the utility of Galangin in clinical settings.

Abbreviations

Gal	Galangin
TNBC	Triple-negative breast cancer
EMT	Epithelial to mesenchymal transition
DNMT	DNA Methyl transferase
HAT	Histone Acyl Transferase
IC ₅₀	Inhibitory Concentration
PR	Progesterone receptor
ER	Estrogen receptor
HER2	Human epidermal growth factor receptor 2
HDACi	HDAC inhibitor
PARP	Poly (ADP-ribose) polymerases
PTEN	Phosphatase and TENSin homolog deleted on chromosome 10
PI3K	Phosphatidylinositol 3-kinase
mTOR	Mammalian target of rapamycin
SAHA	Suberoylanilide hydroxamic acid
CM-H ₂ DCFDA-5-(and-6)	chloromethyl-2',7'-dichlorofluorescein diacetate acetyl ester
TRAIL-TNF	Related apoptosis-inducing ligand
FITC	fluorescein isothiocyanate
MTT-3-(4,5-Dimethylthiazol-2-yl)-2,5	diphenyltetrazoliumbromide
HRP	Horseradish peroxidase
DMSO	Dimethyl Sulphoxide
ROS	Reactive oxygen species
DAPI-4',6	Diamidino-2-phenylindole
PBS	Phosphate buffer saline
FACS	Fluorescence-activated cell sorting
PVDF	Polyvinylidene fluoride
TBST	Tris Buffer saline containing tween
MMP2/9	Matrix metalloproteinases
DMEM	Dulbecco's Modified Eagle Medium
FBS	Foetal bovine serum
G + S	Gal + SAHA
MMP	Mitochondrial membrane potential
IF	Immunofluorescence

Supplementary Information

The online version contains supplementary material available at <https://doi.org/10.1186/s12964-025-02174-3>.

Supplementary Material 1

Acknowledgements

SN sincerely acknowledges to SERB (File No. EEQ/2019/000027) and ICMR (File no.45/33/2022-DDI/BMS) for providing JRF and SRF during Ph.D. RNG acknowledges to SERB (File No. EEQ/2023/000151) and RUSA Phase 2 grant of SPPU Pune.

Author contributions

RNG designed the study and SN have performed all in-vitro cell culture experiments, and wrote the manuscript. SN, NMK and MP performed in-vitro experiments. RB and MS performed in-vivo studies. RNG drafted the manuscript.

Data availability

No datasets were generated or analysed during the current study.

Declarations**Competing interests**

The authors declare no competing interests.

Author details

¹Department of Biotechnology, Savitribai Phule Pune University Pune, Pune, Maharashtra (MS) 411007, India

²National Centre for Cell Science, Pune 411007, India

³Department of Biotechnology, Savitribai Phule Pune University (SPPU), Pune 411007, India

Received: 12 September 2024 / Accepted: 24 March 2025

Published online: 02 April 2025

References

- Zhu S, Wu Y, Song B, Yi M, Yan Y, Mei Q, Wu K. Recent advances in targeted strategies for triple-negative breast cancer. *J Hematol Oncol*. 2023;16(1):100.
- Wu HT, Lin J, Liu YE, Chen HF, Hsu KW, Lin SH, Peng KY, Lin KJ, Hsieh CC, Chen DR. Luteolin suppresses androgen receptor-positive triple-negative breast cancer cell proliferation and metastasis by epigenetic regulation of MMP9 expression via the AKT/mTOR signaling pathway. *Phytomedicine*. 2021;81:153437.
- Mei XY, Zhang JN, Jia WY, Lu B, Wang MN, Zhang TY, Ji LL. Scutellarin suppresses triple-negative breast cancer metastasis by inhibiting TNF α -induced vascular endothelial barrier breakdown. *Acta Pharmacol Sin*. 2022;43(10):2666–77.
- Zam W, Khadour A. Impact of phytochemicals and dietary patterns on epigenome and cancer. *Nutr Cancer*. 2017;69:184–200.
- Khan H, Belwal T, Efferth T, Farooqi AA, Sanches-Silva A, Vacca RA, Nabavi SF, Khan F, Prasad Devkota H, Barreca D, Sureda A, Tejada S, Dacrema M, Daglia M, Suntar I, Xu S, Ullah H, Battino M, Giampieri F, Nabavi SM. Targeting epigenetics in cancer: therapeutic potential of flavonoids. *Crit Rev Food Sci Nutr*. 2021;61(10):1616–39.
- Fatima N, Baqri SSR, Bhattacharya A, Koney NK, Husain K, Abbas A, Ansari RA. Role of flavonoids as epigenetic modulators in cancer prevention and therapy. *Front Genet*. 2021;12:758733.
- Selvakumar P, Badgeley A, Murphy P, Anwar H, Sharma U, Lawrence K, Lakshmikuttyamma A. Flavonoids and other polyphenols act as epigenetic modifiers in breast cancer. *Nutrients*. 2020;12(3):761.
- Nowrasteh G, Zand A, Raposa LB, Szabó L, Tomesz A, Molnár R, Kiss I, Orsós Z, Gerencsér G, Gyöngyi Z, Varjas T. Fruit extract, rich in polyphenols and flavonoids, modifies the expression of *DNMT* and *HDAC* genes involved in epigenetic processes. *Nutrients*. 2023;15(8):1867.
- Rahimian A, Barati G, Mehrandish R, Mellati AA. Inhibition of histone deacetylases reverses Epithelial-Mesenchymal transition in Triple-Negative breast cancer cells through a slug mediated mechanism. *Mol Biol (Mosk)*. 2018;52(3):474–81.
- Gao M, Lai K, Deng Y, Lu Z, Song C, Wang W, Xu C, Li N, Geng Q. Eriocitrin inhibits epithelial-mesenchymal transformation (EMT) in lung adenocarcinoma cells via triggering ferroptosis. *Aging*. 2023;15(19):10089–104.
- Lin YS, Tsai PH, Kandaswami CC, Cheng CH, Ke FC, Lee PP, Hwang JJ, Lee MT. Effects of dietary flavonoids, Luteolin, and Quercetin on the reversal of epithelial-mesenchymal transition in A431 epidermal cancer cells. *Cancer Sci*. 2011;102(10):1829–39.
- Tomooka F, Kaji K, Nishimura N, Kubo T, Iwai S, Shibamoto A, Suzuki J, Kitagawa K, Namisaki T, Akahane T, Mitoro A, Yoshiji H. Sulforaphane potentiates Gemcitabine-Mediated Anti-Cancer effects against intrahepatic cholangiocarcinoma by inhibiting HDAC activity. *Cells*. 2023;12(5):687.
- Ting Lu CZ, Fan Z. Cardamonin suppressed the migration, invasion, epithelial mesenchymal transition (EMT) and lung metastasis of colorectal cancer cells by down-regulating ADRB2 expression. *Pharm Biol*. 2022;60:1011–21.
- Zhang G, Li Z, Dong J, Zhou W, Zhang Z, Que Z, Zhu X, Xu Y, Cao N, Zhao A. Acacetin inhibits invasion, migration and TGF- β 1-induced EMT of gastric cancer cells through the PI3K/Akt/Snail pathway. *BMC Complement Med Ther*. 2022;22(1):10.
- Maleki Dana P, Sadoughi F, Asemi Z, Yousefi B. The role of polyphenols in overcoming cancer drug resistance: a comprehensive review. *Cell Mol Biol Lett*. 2022;27(1):1.
- Donovan MG, Selmin OL, Doetschman TC, Romagnolo DF. Epigenetic activation of *BRCA1* by genistein in vivo and triple negative breast cancer cells linked to antagonism toward Aryl hydrocarbon receptor. *Nutrients*. 2019;11(11):2559.
- Ashrafizadeh M, Zarrabi A, Saberifar S, Hashemi F, Hushmandi K, Hashemi F, Moghadam ER, Mohammadinejad R, Najafi M, Garg M. Nobiletin in cancer therapy: how this plant Derived-Natural compound targets various oncogene and Onco-Suppressor pathways. *Biomedicines*. 2020;8(5):110.
- Adinew GM, Taka E, Mendonca P, Messeha SS, Soliman KFA. The anticancer effects of flavonoids through MiRNAs modulations in Triple-Negative breast cancer. *Nutrients*. 2021;13(4):1212.
- Xiong Y, Lai X, Xiang W, Zhou J, Han J, Li H, Deng H, Liu L, Peng J, Chen L. Galangin (GLN) suppresses proliferation, migration, and invasion of human glioblastoma cells by targeting Skp2-Induced Epithelial-Mesenchymal transition (EMT). *Onco Targets Ther*. 2020;13:9235–44.
- Ren K, Zhang W, Wu G, Ren J, Lu H, Li Z, Han X. Synergistic anti-cancer effects of Galangin and Berberine through apoptosis induction and proliferation Inhibition in oesophageal carcinoma cells. *Biomed Pharmacother*. 2016;84:1748–59.
- Song W, Yan CY, Zhou QQ, Zhen LL. Galangin potentiates human breast cancer to apoptosis induced by TRAIL through activating AMPK. *Biomed Pharmacother*. 2017;89:845–56.
- Choudhari J, Nimma R, Nimal SK, Totakura Venkata SK, Kundu GC, Gacche RN. *Prosopis juliflora* (Sw.) DC phytochemicals induce apoptosis and inhibit cell proliferation signaling pathways, EMT, migration, invasion, angiogenesis and stem cell markers in melanoma cell lines. *J Ethnopharmacol*. 2023;312:116472.
- Kumbhar N, Nimal S, Patil D, Kaiser VF, Haupt J, Gacche RN. Repurposing of Nephilysin inhibitor 'scubitrilat' as an anti-cancer drug by modulating epigenetic and apoptotic regulators. *Sci Rep*. 2023;13(1):9952.
- Nimal S, Kumbhar N, Saruchi, Rathore S, Naik N, Paymal S, Gacche RN. Apigenin and its combination with Vorinostat induces apoptotic-mediated cell death in TNBC by modulating the epigenetic and apoptotic regulators and related MiRNAs. *Sci Rep*. 2024;14(1):9540.
- Chou TC. Theoretical basis, experimental design, and computerized simulation of synergism and antagonism in drug combination studies. *Pharmacol Rev*. 2006;58(3):621–81.
- Prasad CP, Chaurasiya SK, Guilmain W, Andersson T. WNT5A signaling impairs breast cancer cell migration and invasion via mechanisms independent of the epithelial-mesenchymal transition. *J Exp Clin Cancer Res*. 2016;35(1):144.
- Utage BG, Patole MS, Nagvenkar PV, Kamble SS, Gacche RN. *Prosopis juliflora* (Sw.), DC induces apoptosis and cell cycle arrest in triple negative breast cancer cells: *in vitro* and *in vivo* investigations. *Oncotarget*. 2018;9(54):30304–30323. doi: 10.18632/oncotarget.25717. Erratum in: *Oncotarget*. 2018; 9(68):33050.
- Conner SJ, Guarin JR, Le TT, Fatherree JP, Kelley C, Payne SL, Parker SR, Bloomer H, Zhang C, Salhany K, McGinn RA, Henrich E, Yui A, Srinivasan D, Borges H, Oudin MJ. Cell morphology best predicts tumorigenicity and metastasis in vivo across multiple TNBC cell lines of different metastatic potential. *Breast Cancer Res*. 2024;26(1):43.
- Brown LJ, Achinger-Kawecka J, Portman N, Clark S, Stirzaker C, Lim E. Epigenetic therapies and biomarkers in breast cancer. *Cancers (Basel)*. 2022;14(3):474.
- Ensenyat-Mendez M, Solivellas-Pieras M, Llinàs-Arias P, Íñiguez-Muñoz S, Baker JL, Marzese DM, DiNome ML. Epigenetic profiles of Triple-Negative breast cancers of African American and white females. *JAMA Netw Open*. 2023;6(10):e2335821.
- Lev S. Targeted therapy and drug resistance in triple-negative breast cancer: the EGFR axis. *Biochem Soc Trans*. 2020;48(2):657–65.
- So JY, Ohm J, Lipkowitz S, Yang L. Triple negative breast cancer (TNBC): Non-genetic tumor heterogeneity and immune microenvironment: emerging treatment options. *Pharmacol Ther*. 2022;237:108253.

33. Geurts VCM, Balduzzi S, Steenbruggen TG, Linn SC, Siesling S, Badve SS, DeMichele A, Ignatiadis M, Leon-Ferre RA, Goetz MP, Wolff AC, Klar N, Michiels S, Loi S, Adams S, Horlings HM, Sonke GS, Salgado R, Kok M. Tumor-Infiltrating lymphocytes in patients with stage I Triple-Negative breast cancer untreated with chemotherapy. *JAMA Oncol.* 2024;10(8):1077–86.
34. Gao S, Zhang X, Liu J, Ji F, Zhang Z, Meng Q, Zhang Q, Han X, Wu H, Yin Y, Lv Y, Shi W. Icarin induces Triple-Negative breast cancer cell apoptosis and suppresses invasion by inhibiting the JNK/c-Jun signaling pathway. *Drug Des Devel Ther.* 2023;17:821–36.
35. Wang X, Zhang L, Si H. Combining Luteolin and Curcumin synergistically suppresses triple-negative breast cancer by regulating IFN and TGF- β signaling pathways. *Biomed Pharmacother.* 2024;178:117221.
36. Lin Y, Li L, Huang H, Wen X, Zhang Y, Zhang R, Huang W. Vitexin inhibits TNBC progression and metastasis by modulating macrophage polarization through EGFR signaling. *J Immunother.* 2024;47(8):303–12.
37. Jiang P, Jiang W, Li X, Zhu Q. Combination of Formononetin and Sulforaphane natural drug repress the proliferation of cervical cancer cells via impeding PI3K/AKT/mTOR pathway. *Appl Biochem Biotechnol.* 2024;196(10):6726–44.
38. Yang Z, Liu H, Song Y, Gao N, Gao P, Hui Y, Li Y, Fan T. Luteolin enhances drug chemosensitivity by downregulating the FAK/PI3K/AKT pathway in Paclitaxel-resistant esophageal squamous cell carcinoma. *Int J Mol Med.* 2024;54(3):77.
39. Pai JT, Chen XH, Leu YL, Weng MS. Propolis G-Suppressed Epithelial-to-Mesenchymal transition in Triple-Negative breast cancer cells via glycogen synthase kinase 3 β -Mediated snail and HDAC6-Regulated vimentin degradation. *Int J Mol Sci.* 2022;23(3):1672.
40. Selmin OI, Donovan MG, Stillwater BJ, Neumayer L, Romagnolo DF. Epigenetic regulation and dietary control of triple negative breast cancer. *Front Nutr.* 2020;7:159.
41. Galkin F, Kovalchuk O, Koldasbayeva D, Zhavoronkov A, Bischof E. Stress, diet, exercise: common environmental factors and their impact on epigenetic age. *Ageing Res Rev.* 2023;88:101956.
42. Sarfraz A, Rasul A, Sarfraz I, Shah MA, Hussain G, Shafiq N, Masood M, Adem S, Sarker SD, Li X. Hispolon: A natural polyphenol and emerging cancer killer by multiple cellular signaling pathways. *Environ Res.* 2020;190:110017.
43. Yang X, Wang Q, Zhang X, Li L, Cao X, Zhou L, Huang Y, Sun G, Chen Y. Purple Yam polyphenol extracts exert anticolicitis and anticolicitis-Associated colorectal cancer effects through inactivation of NF- κ B/p65 and STAT3 signaling pathways. *J Agric Food Chem.* 2023;71(32):12177–89.
44. Islam MA, Medha MM, Nahar AU, Al Fahad MA, Siraj MA, Seidel V. Cancer protective role of selected dietary polyphenols via modulating Keap1/Nrf2/ARE and interconnected signaling pathways. *Nutr Cancer.* 2023;75(4):1065–102.
45. Konstantinou EK, Panagiotopoulos AA, Argyri K, Panoutsopoulos GI, Dimitriou M, Gioxari A. Molecular pathways of Rosmarinic acid anticancer activity in Triple-Negative breast cancer cells: A literature review. *Nutrients.* 2023;16(1):2.
46. Sharma M, Arora I, Chen M, Wu H, Crowley MR, Tollefsbol TO, Li Y. Therapeutic effects of dietary soybean genistein on Triple-Negative breast cancer via regulation of epigenetic mechanisms. *Nutrients.* 2021;13(11):3944.
47. Tuli HS, Sak K, Adhikary S, Kaur G, Aggarwal D, Kaur J, Kumar M, Parashar NC, Parashar G, Sharma U, Jain A. Galangin: A metabolite that suppresses anti-neoplastic activities through modulation of oncogenic targets. *Exp Biol Med (Maywood).* 2022;247(4):345–59.
48. Jiang W, Xia T, Liu C, Li J, Zhang W, Sun C. Remodeling the epigenetic landscape of cancer-Application potential of flavonoids in the prevention and treatment of cancer. *Front Oncol.* 2021;11:705903.
49. Kaur S, Mendonca P, Soliman KFA. The anticancer effects and therapeutic potential of Kaempferol in Triple-Negative breast cancer. *Nutrients.* 2024;16(15):2392.
50. Afzal M, Alarifi A, Karami AM, Ayub R, Abdul NAY, Saeed WS, Muddasir M. Antiproliferative mechanisms of a polyphenolic combination of Kaempferol and Fisetin in Triple-Negative breast cancer cells. *Int J Mol Sci.* 2023;24(7):6393.
51. Wang C, Liu B, Dan W, Wei Y, Li M, Guo C, Zhang Y, Xie H. Liquiritigenin inhibits the migration, invasion, and EMT of prostate cancer through activating ER stress. *Arch Biochem Biophys.* 2024;761:110184.
52. Zhu Z, Wang H, Qian X, Xue M, Sun A, Yin Y, Tang J, Zhang J. Inhibitory impact of Cinobufagin in Triple-Negative breast cancer metastasis: involvements of macrophage reprogramming through upregulated MME and inactivated FAK/STAT3 signaling. *Clin Breast Cancer.* 2024;24(4):e244–ee2571.
53. Chen KC, Hsu WH, Ho JY, Lin CW, Chu CY, Kandaswami CC, Lee MT, Cheng CH. Flavonoids Luteolin and Quercetin inhibit RPS19 and contributes to metastasis of cancer cells through c-Myc reduction. *J Food Drug Anal.* 2018;26(3):1180–91.
54. Yang B, Bai H, Sa Y, Zhu P, Liu P. Inhibiting EMT, stemness and cell cycle involved in baicalin-induced growth inhibition and apoptosis in colorectal cancer cells. *J Cancer.* 2020;11(8):2303–17.
55. Liang X, Wang P, Yang C, Huang F, Wu H, Shi H, Wu X. Galangin inhibits gastric cancer growth through enhancing STAT3 mediated ROS production. *Front Pharmacol.* 2021;12:646628.
56. Cho Y, Park MN, Choi M, Upadhyay TK, Kang HN, Oh JM, Min S, Yang JU, Kong M, Ko SG, Rahman MA, Harrath AH, Kim B. Sulforaphane regulates cell proliferation and induces apoptotic cell death mediated by ROS-cell cycle arrest in pancreatic cancer cells. *Front Oncol.* 2024;14:1442737.
57. Guha S, Talukdar D, Mandal GK, Mukherjee R, Ghosh S, Naskar R, Saha P, Murmu N, Das G. Crude extract of *Ruellia tuberosa* L. flower induces intracellular ROS, promotes DNA damage and apoptosis in triple negative breast cancer cells. *J Ethnopharmacol.* 2024;332:118389.
58. Xu S, Sun X, Luo L, Yang Y, Guo Q, Tang S, Li BZ, Han Y, Gan J, Yang W, Zhang F, Liu X, Sun Y, He C, Liu J, Zuo M, Zhu D, Wu W. XS-2, a novel potent dual PI3K/mTOR inhibitor, exhibits high in vitro and in vivo anti-breast cancer activity and low toxicity with the potential to inhibit the invasion and migration of triple-negative breast cancer. *Biomed Pharmacother.* 2022;155:113537.

Publisher's note

Springer Nature remains neutral with regard to jurisdictional claims in published maps and institutional affiliations.